

Contribution from the Laboratoire de Cristallographie aux Rayons X, Université de Genève, CH-1211 Genève 4, Switzerland, Institut für Reaktortechnik, ETH Zürich, CH-5303 Würenlingen, Switzerland, and Département de Chimie Minérale, Analytique et Appliquée, Université de Genève, CH-1211 Genève 4, Switzerland

Dimagnesium Iron(II) Hydride, Mg_2FeH_6 , Containing Octahedral FeH_6^{4-} Anions

J.-J. DIDISHEIM,[†] P. ZOLLIKER, K. YVON,* P. FISCHER, J. SCHEFER, M. GUBELMANN, and A. F. WILLIAMS

Received September 7, 1983

The ternary metal hydride Mg_2FeH_6 and its deuteride have been prepared as dark green crystalline solids by a sintering technique at $\sim 500^\circ C$ under 20–120 atm of H_2 (D_2) pressure. X-ray and neutron powder diffraction analysis showed cubic symmetry ($a = 6.443$ (1) Å; deuteride $a = 6.430$ (1) Å) and the K_2PtCl_6 structure type. The Fe–H bond distances in the deuteride at 293 K are 1.556 (5) Å. Mössbauer, Raman, and IR measurements show the presence of octahedral low-spin $[FeH_6]^{4-}$ ions. The heat of dissociation of the hydride was measured from pressure–composition isotherms and found to be 98 (3) kJ/mol of H_2 .

Introduction

In a recent study of the hydrogen storage material Mg_2NiH_4 it was suggested that the maximal hydrogen concentration of this compound is mainly limited by electronic factors and that structurally related compounds having more than four H atoms per formula unit could possibly be stabilized if Ni was replaced by metals earlier in the 3d series.¹ Attempts to prepare such compounds by partially replacing Ni by V, Cr, Mn, Fe, and Co in the binary phase Mg_2Ni have been reported,² but the alloys obtained have so far failed to yield hydrides having more than four H atoms per formula unit.

In this paper we report the preparation, structure, and properties of the iron-based hydride Mg_2FeH_6 . This compound contains six H atoms per formula unit and shows a considerably better hydrogen-to-metal weight ratio than the nickel-based hydride Mg_2NiH_4 . Also, its hydrogen concentration per unit volume is exceptionally high, exceeding for instance that of MgH_2 by about 40%. The preparation was carried out from the elements by using a sintering technique similar to that used for the synthesis of the closely related ruthenium-based hydrides M_2RuH_6 ($M = Ca, Sr, Eu, Yb$).^{3–5} A preliminary account of the results presented in this article has appeared elsewhere.⁶

Experimental Section

Synthesis. Magnesium powder (Fluka, purum p.a., 50–150 mesh) and iron powder (Alfa, 60 mesh) were mixed in a 2:1 Mg:Fe atomic ratio and pressed under 10 kbar to cylindrical pellets measuring 5–10 mm in height and weighing about 2 g each. The pellets were enclosed in stainless-steel containers with a filter cap allowing gas exchange, placed in an autoclave, and treated for 2–10 days at various temperatures (450–520 °C) and hydrogen pressures (20–120 bar). After cooling to room temperature, the containers were taken out of the autoclave and the amount of absorbed hydrogen was measured gravimetrically.

The sintered ("unpurified") samples, which contained up to 50% magnesium dihydride, magnesium, and iron impurity phases, were purified as follows. The finely ground powder was suspended in chloroform and magnetically stirred. The free iron adhered to the magnetic stirrer and could be removed mechanically. The remaining products were dried and suspended in purified 1,2-dibromoethane. This liquid has a density of 2.15 g·cm⁻³, so that Mg (1.74 g·cm⁻³) and MgH_2 (1.42 g·cm⁻³) floated to the surface of the tube and could be removed. The remaining dark green product at the bottom of the tube was dried and analyzed (called "purified sample" hereafter). It consisted of a green powder that was quite stable in air but decomposed slowly in moist air over a period of some weeks. The total amount of impurity phases left (mainly MgH_2 and Fe) was estimated to be less than 10%.

Analysis. The sample was dissolved in warm dilute HCl containing a little hydrogen peroxide. Iron was determined directly by complexometric titration with EDTA using sulfosalicylic acid as an indicator, and magnesium by EDTA titration after extraction of the iron with cupferron into 1:1 toluene/isoamyl alcohol.⁷ Results: 48.0% Fe (calcd 50.5%), 43.2% Mg (calcd 44.0%); Mg:Fe mole ratio 2.06. Densities were measured by flotation in CH_2I_2 /1,2-dibromoethane mixtures.

Physical Measurements. X-ray powder diffraction data were obtained with a Guinier camera (Cu $K\alpha$ radiation), a Debye–Scherrer camera (V-filtered Cr $K\alpha$ radiation), and a Philips diffractometer (Ni-filtered Cu $K\alpha$ radiation). Neutron diffraction spectra were recorded at room temperature for a purified deuteride sample on a two-axis diffractometer at the reactor SAPHIR at IRT, Würenlingen. The sample weighed about 1.5 g, and it was enclosed under argon in an indium-sealed vanadium container of 1-cm diameter.

Infrared spectra were obtained in the range 4000–240 cm⁻¹ by using samples in KBr disks. A Spectra Physics argon ion laser and a SPEX 1403 double monochromator were used to obtain Raman spectra from powder samples sealed in glass capillaries. Mössbauer spectra were obtained at room temperature by using a constant-acceleration spectrometer calibrated with a metallic iron foil. The spectra were fitted to a Lorentzian curve by the use of the least-squares procedure of Stone.⁸

Magnetization measurements were made on both purified and unpurified samples at temperatures of 300 and 4.2 K, using the Faraday method and a magnetometer equipped with a superconducting coil.

Results

After the Mg/Fe mixtures were sintered in hydrogen atmosphere, the samples showed a weight increase ranging between 2.8% and 4.6%, depending on experimental conditions. Optimal conditions for hydrogen absorption were found at temperatures around 500 °C and pressures around 60 bar. The samples that were sintered under deuterium pressure showed weight increases approximately twice as high, indicating similar concentrations of absorbed deuterium. When the containers were opened, it was found that the pellets which had absorbed more than about 3.3 wt % hydrogen had disintegrated into a fine greenish powder. As shown by X-ray and neutron diffraction analysis and by spectroscopic measure-

* To whom correspondence should be addressed at the Laboratoire de Cristallographie aux Rayons X, Université de Genève.

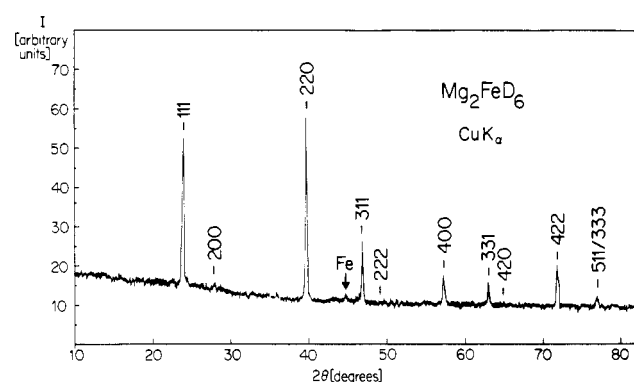
[†] Present address: Department of Materials Science and Engineering, Massachusetts Institute of Technology, Cambridge, MA 02139.

- (1) Yvon, K.; Schefer, J.; Stucki, F. *Inorg. Chem.* **1981**, *20*, 2776.
- (2) Ono, S.; Nomura, K.; Suzuki, K.; Higano, S.; Kamino, K. *Trans. Jpn. Inst. Met., Suppl.* **1980**, *21*, 361.
- (3) Moyer, R. O., Jr.; Stanitski, C.; Tanaka, J.; Kay, M. I.; Kleinberg, R. *J. Solid State Chem.* **1971**, *3*, 541.
- (4) Thompson, J. S.; Moyer, R. O., Jr.; Lindsay, R. *Inorg. Chem.* **1975**, *14*, 1866.
- (5) Lindsay, R.; Moyer, R. O., Jr.; Thompson, J. S.; Kuhn, D. *Inorg. Chem.* **1976**, *15*, 3050.
- (6) Didisheim, J.-J.; Yvon, K.; Fischer, P.; Schefer, J.; Gubelmann, M.; Williams, A. F. *Z. Kristallogr.* **1983**, *162*, 61.
- (7) Fritz, J. S.; Johnson-Richard, M.; Sutton-Bystroff, A. *Anal. Chem.* **1957**, *29*, 577.
- (8) Appendix to: Stone, A. J. *J. Chem. Soc. A* **1967**, 1966.

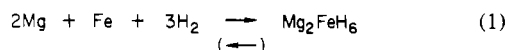
Table I. Comparison between Observed and Calculated X-ray Powder Patterns for Mg_2FeD_6 ^a

<i>hkl</i>	$1/d^2_{\text{obsd}}$, \AA^{-2}	$1/d^2_{\text{calcd}}$, \AA^{-2}	I_{obsd}	I_{calcd}
111	0.0735	0.0726	80	85.7
200		0.0967	3	1.5
220	0.1946	0.1936	100	100.0
311	0.2671	0.2660	33	31.7
222		0.2903	0	0.3
400	0.3882	0.3867	16	15.8
331	0.4609	0.4596	12	10.0
420		0.4836	0	0.4
422	0.5809	0.5801	22	22.4
511	0.6535	0.6535	6	4.6
333				1.5

^a The observed $1/d^2$ values were obtained from a Debye-Scherrer photograph (camera circumference 360 mm) taken with V-filtered $\text{Cr K}\alpha$ radiation. Observed intensities correspond to the peak height of the lines in Figure 1, scaled to 100 for the strongest reflection. Calculated intensities are from the program LAZY-PULVERIX⁹ (see text for the structural parameters).

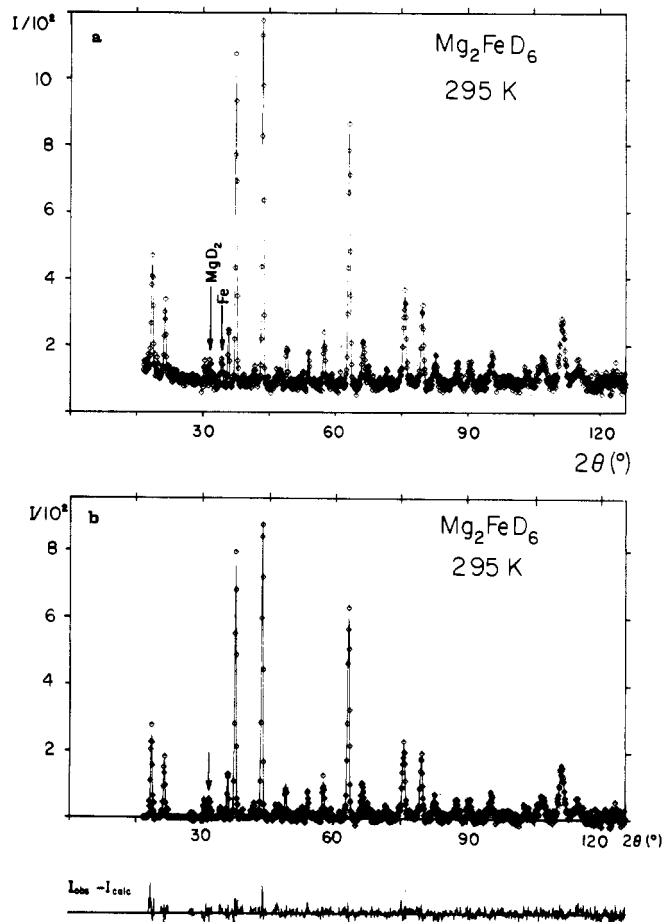
**Figure 1.** X-ray powder pattern of a purified Mg_2FeD_6 sample taken on a Philips diffractometer with Ni-filtered $\text{Cu K}\alpha$ radiation. Scanning speed $1^\circ 2\theta \text{ min}^{-1}$.

ments (see below), the powder contained a new ternary metal hydride phase of composition Mg_2FeH_6 , which was formed according to reaction 1. However, due to the presence of



significant amounts of magnesium hydride (MgH_2) and unreacted Mg and Fe metal in the sintered samples, the exact composition of this phase and in particular its H concentration were not immediately apparent.

X-ray and Neutron Diffraction. Guinier photographs of unpurified samples showed the presence of 5–30 atom % unreacted iron, depending on sample and preparation conditions, and about twice this amount of magnesium and/or magnesium hydride. The powder pattern remaining after subtraction of the diffraction lines due to Fe, Mg, and MgH_2 was ascribed to the ternary hydride phase. It was indexed on the basis of a face-centered cubic cell with lattice parameter $a = 6.443$ (1) \AA (hydride), 6.430 (1) \AA (deuteride). The same parameter values (within error limits) were found for the purified samples and also for all other samples, which were prepared under different experimental conditions, thus indicating the absence of a detectable range of homogeneity for this phase. A comparison with a calculated powder diffraction diagram (Table I) showed that its metal atom arrangement was of the fluorite type (space group $Fm\bar{3}m$ (No. 225);¹⁰ Mg in $8c$ ($1/4, 1/4, 1/4$); Fe in $4a$ (0, 0, 0)). A diffractometer intensity profile taken

**Figure 2.** (a) Neutron powder diffraction pattern of a purified Mg_2FeD_6 sample at room temperature, after correction for absorption. Wavelength: $\lambda = 1.188$ (1) \AA . The strongest peaks of the Fe and MgD_2 impurity phases are marked by arrows. (b) Same pattern as in part a, after subtraction of the background and the contributions due to the Fe impurity phase. The strongest line of the MgD_2 impurity phase is marked by an arrow. The full lines correspond to the calculated profile (top) and the difference pattern $I_{\text{obsd}} - I_{\text{calcd}}$ (bottom).

on the purified deuteride sample is represented in Figure 1. Except for one small peak due to the Fe impurity (marked by an arrow) and a few very small peaks due to binary MgD_2 (visible only on Guinier photographs) all peaks could be attributed to the ternary phase, and their intensity sequence corresponded closely to that of the high-temperature phase of Mg_2NiH_4 ,^{11,12} which has the same metal atom arrangement. Assuming that the structure contains six hydrogen (deuterium) atoms per formula unit, the calculated density of Mg_2FeH_6 is $2.74 \text{ g}\cdot\text{cm}^{-3}$ and that of Mg_2FeD_6 is $2.91 \text{ g}\cdot\text{cm}^{-3}$. Both values are in good agreement with the experimental densities of 2.73 (3) $\text{g}\cdot\text{cm}^{-3}$ (hydride) and 2.87 (3) $\text{g}\cdot\text{cm}^{-3}$ (deuteride), as measured on purified samples.

The concentration and distribution of the deuterium atoms in the structure was investigated by a high-resolution neutron diffraction experiment [$[(\sin \theta)/\lambda]_{\text{max}} = 0.69 \text{ \AA}^{-1}$] on a purified deuteride sample. Its diffraction pattern is shown in Figure 2a. After subtraction of the background, the contribution of the Fe impurity phase was estimated from the intensities of isolated Bragg peaks (see arrow in Figure 2a) and then subtracted from the experimental pattern. The remaining intensity profile was assumed to be due to the ternary $\text{Mg}_2\text{-FeD}_6$ phase and a very small amount of binary MgD_2 (see

(9) Yvon, K.; Jeitschko, W.; Parthé, E. *J. Appl. Crystallogr.* **1977**, *10*, 73.

(10) "International Tables for X-ray Crystallography"; Kynoch Press: Birmingham, England, 1969; Vol. I.

(11) Gavra, Z.; Mintz, M. H.; Kimmel, G.; Hadari, Z. *Inorg. Chem.* **1979**, *18*, 3595.(12) Ono, S.; Hayakawa, H.; Suzuki, A.; Nomura, K.; Nishimiya, N.; Tabata, T. *J. Less-Common Met.* **1983**, *88*, 63.

Table II. Neutron Diffraction Results for Mg₂FeD₆ (Space Group *Fm3m*^{10,a})

Atomic Coordinates and Isotropic Temperature Factors				
	<i>x</i>	<i>y</i>	<i>z</i>	<i>B</i> , Å ²
Mg (8c)	1/4	1/4	1/4	0.5 (1)
Fe (4a)	0	0	0	0.15 (7)
D (24e)	0.2420 (7)	0	0	1.6 (1)

no. of deuterium atoms per formula unit: $n_D = 6.2$ (1)
R factors:^b $R_F = 0.067$ (40 reflcns); $R_D = 0.27$
 lattice constant: $a = 6.437$ (5) Å ($a_{X\text{-ray}} = 6.430$ (1) Å)

^a Figures in parentheses are esd's calculated by the Rietveld program,¹³ except for the esd of *a* (estimated from the uncertainty of λ). ^b See ref 13 for definition.

arrow in Figure 2b). Their structures were refined with the Rietveld program¹³ as modified for simultaneous treatment of two phases.¹⁴ The parameters refined for MgD₂ (rutile type) were the positional coordinates of the D atoms and the concentration of this phase in the sample. For Mg₂FeD₆, the D atoms were placed on position 24e (*x*, 0, 0) of space group *Fm3m* with *x* ~ 0.24, corresponding to the anion positions in the K₂PtCl₆ structure type. Its coordinate (*x*) and occupancy (n_D) were refined together with three independent temperature factors, B_{Fe} , B_{Mg} , and B_D , an overall scale factor, and the usual profile parameters (cell constants, half-widths, and zero-point correction). During refinement all correlation coefficients between the different structural parameters and in particular that between the occupancy factor and the temperature factor of the deuterium atom site remained small (less than 0.5). The results of the refinement are summarized in Table II, and a comparison between the observed and calculated diffraction profiles is shown in Figure 2b.

Clearly, the neutron diffraction experiment confirms the K₂PtCl₆ structure type and shows that the D atom positions do not differ greatly from those in the isostructural deuteride Sr₂RuD₆.³ In particular the occupancy factor of the D atom site in Mg₂FeD₆ is close to 6 ($n_D = 6.2$ (1)), which excludes a significant fraction of the iron atoms from being surrounded by less than six D atoms or nonoctahedral D atom configurations. As will be shown below, the spectroscopic data are in complete agreement with this structural model and show that any possible deviation from Mg₂FeD₆ stoichiometry must be even smaller than that implied by the accuracy of the neutron diffraction data.

The main structural unit of Mg₂FeD₆ is represented in Figure 3. It shows the octahedral FeD₆ group, which is surrounded by eight Mg atoms in a cubic configuration. These groups are arranged on a fcc lattice such that each Mg atom is tetrahedrally surrounded by 4 FeD₆ groups and has 12 D atoms as nearest neighbors. The metal-deuterium bond distances are $d(Fe-D) = 1.556$ (5) Å and $d(Mg-D) = 2.2739$ (3) Å, and the shortest separations between the deuterium atoms within (intra) and between (inter) the FeD₆ groups are $d^{intra}(D-D) = 2.201$ (6) Å and $d^{inter}(D-D) = 2.346$ (6) Å. A preliminary neutron diffraction study of a nonpurified sample of Mg₂FeH₆ showed the same structure type and similar interatomic distances.

Mössbauer Spectroscopy. The Mössbauer spectrum at room temperature of a purified sample of Mg₂FeD₆ shows a sharp single line ($\Gamma = 0.27$ (2) mm·s⁻¹) with an isomer shift of +0.02 (1) with respect to metallic iron. Slight traces of metallic iron could be detected, with a total intensity corresponding to 6.5% of the total absorption. A spectrum taken at 100 K showed no change in line width, excluding the possibility of dynamic

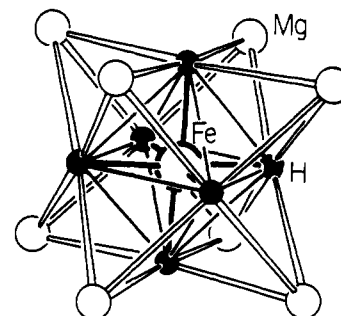


Figure 3. Structural unit of Mg₂FeH₆ having the K₂PtCl₆ structure type.

disorder of the deuterium atoms. The hydride gives a similar spectrum.

The absence of any detectable quadrupole splitting requires the coordination of the iron to be cubic, either octahedral or tetrahedral, and excludes the possibility of a five-coordinate species, which would show a large quadrupole splitting.¹⁵ The distinction between octahedral and tetrahedral coordination may be made by vibrational spectroscopy (see below).

The isomer shift is typical for low-spin iron(II)¹⁶ or iron(III),¹⁷ but the latter may be excluded as iron(III) low-spin complexes generally show a measurable quadrupole splitting. High-spin iron(II) and iron(III) may equally be excluded. A metallic system might be expected to show a similar isomer shift, but we do not consider this to be at all probable as the compound is olive green and (apart from the Fe-H or Fe-D vibrations) is transparent in the infrared spectrum down to 400 cm⁻¹. Further arguments in favor of low-spin iron(II) are the relatively long metal-metal distances, the observation that many ternary hydride systems appear to obey the 18-electron rule¹ (low spin [FeH₆]⁴⁻ would be another example), and the recent preparation of FeH₆Mg₄X₄(THF)₈ (X = halogen) containing low-spin iron(II).¹⁸ A low-spin d⁶ configuration was previously proposed for ruthenium in M₂RuH₆ from the ⁹⁹Ru Mössbauer spectrum.¹⁹

Vibrational Spectroscopy. The infrared spectrum of Mg₂FeH₆ shows only one strong band at 1720 cm⁻¹, which is shifted to 1262 cm⁻¹ in Mg₂FeD₆. The Raman spectrum of Mg₂FeH₆ shows a medium band at 1870 cm⁻¹, shifted to 1340 cm⁻¹ on deuteration. The ratios of the frequencies for the FeH₆ and FeD₆ species are 1.36 (infrared) and 1.40 (Raman), close to the value expected for the change in reduced mass on deuteration (1.40), and thus confirm the assignment of these bands to Fe-H or Fe-D stretching modes. The infrared absorption band was fairly broad and the Raman spectra fairly weak, but neither showed any trace of unresolved splitting. No trace of a band at the infrared frequency could be observed in the Raman spectrum and vice versa. In agreement with the Mössbauer data, a low-symmetry environment of the iron may therefore be excluded. For tetrahedral (*T_d*) symmetry two bands (*A₁* and *T₂*) are expected in the Raman spectrum, the *T₂* band being also active in the infrared, whereas for octahedral (*O_h*) symmetry the Raman spectrum shows two bands (*A_{1g}* and *E_g*) and the infrared spectrum one band (*T_{1u}*). The absence of bands at the same energy in the infrared and Raman spectra rules out *T_d* symmetry. The failure to observe the second (*E_g*) band in the Raman spectrum is not significant, since this band is frequently more than 1 order of magnitude

(13) Rietveld, H. M. *J. Appl. Crystallogr.* **1969**, *2*, 65.

(14) Werner, P. E.; Salomé, S.; Malmros, G.; Thomas, J. O. *J. Appl. Crystallogr.* **1979**, *12*, 107.

(15) Bancroft, G. M.; Libbey, E. T. *J. Chem. Soc., Dalton Trans* **1973**, 2103.

(16) Bancroft, G. M.; Mays, M. J.; Prater, B. E. *J. Chem. Soc. A* **1970**, 956.

(17) Greenwood, N. N.; Gibb, T. C. "Mössbauer Spectroscopy"; Chapman & Hall: London, 1977; Chapter 7.

(18) Bau, R.; Ho, D. M.; Gibbins, S. G. *J. Am. Chem. Soc.* **1981**, *103*, 4960.

(19) Fernandez, I.; Greatrex, R.; Greenwood, N. N. *J. Chem. Soc., Dalton Trans.* **1980**, 918.

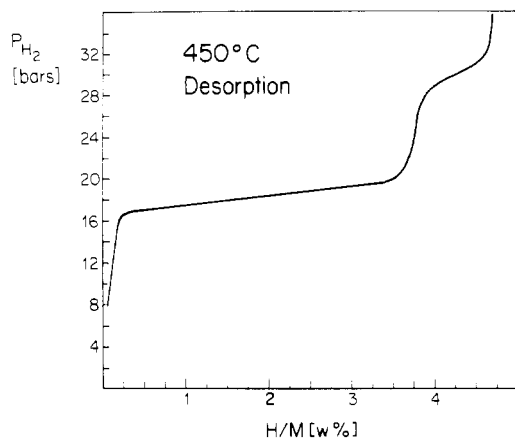


Figure 4. Desorption isotherm of an unpurified Mg_2FeH_6 sample containing Mg_2FeH_6 and MgH_2 .

less intense than the A_{1g} band.²⁰ Two further points may be made in support of O_h symmetry: (i) in T_d the infrared-active frequency T_2 is normally at higher energy than A_1 whereas the opposite is observed for our compound, and (ii) the infrared frequency (T_{1u} in O_h) is, as would be expected, very close indeed to that reported for the antisymmetric H-Fe-H stretch in the low-spin iron(II) complex *trans*- $[\text{FeH}_2(\text{C}_2\text{H}_4(\text{PET}_2)_2)_2]$, 1726 cm^{-1} .²¹

In conclusion, the spectroscopic data are perfectly consistent with the formulation of a low spin $[\text{FeH}_6]^{4-}$ complex, and we can think of no other satisfactory explanation of the data.

Magnetization Measurements. At 4.2 K the magnetization was found to increase steeply as a function of the applied field up to $H \sim 10 \text{ kOe}$ and to level off at values near 18.3 emu/g (unpurified sample) and 2.6 emu/g (purified sample) at fields of $H \sim 40 \text{ kOe}$. At 300 K the magnetization was lower by up to 1.5 emu/g . From the saturation values the amount of full iron was estimated to be $\sim 8.5 \text{ wt } \%$ in the unpurified hydride sample and $\sim 1.5 \text{ wt } \%$ in the purified hydride sample. These values are close to those found by diffraction analysis and desorption measurements (see below). The magnetic behavior of the samples is thus dominated by the free iron present as an impurity, which does not allow us to draw further conclusions on the magnetic properties of Mg_2FeH_6 . The present measurements, however, are consistent with the Mössbauer data, which suggest a diamagnetic low-spin iron(II) complex.

Pressure-Composition Isotherms. The stability of the compounds was measured from pressure-composition isotherms, of which a representative curve is shown in Figure 4. It consists of two plateaus, of which that at $p = 30 \text{ bar}$ corresponds to the desorption of the binary MgH_2 impurity phase²² and that at $p \sim 18 \text{ bar}$ can be ascribed to the desorption of Mg_2FeH_6 . The relatively small inclination of the latter plateau and the steep variations on both sides of it confirm that this compound has only a small range of homogeneity for hydrogen. The enthalpy of formation of Mg_2FeH_6 was determined from pressure-composition isotherms recorded at different temperatures. As shown in Figure 5 the plateau pressures for absorption and desorption vary approximately linearly as a function of reciprocal temperature, according to the relationship $d(\ln p_{\text{H}_2})/d(1/T) = \Delta H/R$ ($R =$ universal gas constant, $\Delta H =$ enthalpy change during reaction 1). The ΔH values derived from these graphs for ab-

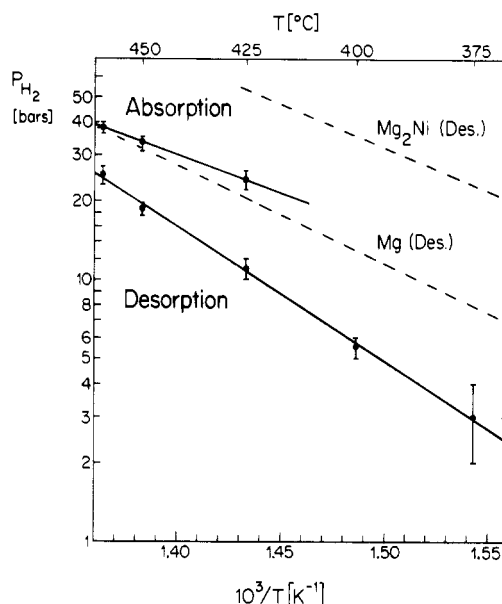


Figure 5. Variation with temperature of the plateau pressure for absorption and desorption of hydrogen for Mg_2FeH_6 . The desorption plateau pressures of MgH_2 and Mg_2NiH_4 are shown for comparison.

sorption and desorption are -55 (3) and 98 (3) kJ/mol of H_2 , respectively. The disproportionation of Mg_2FeH_6 into elemental Mg and Fe upon desorption was revealed by X-ray analysis. It was also found that the hydrogen uptake of the sample decreased by about 35% after four consecutive cycles of absorption and desorption. This indicates the need for compressing the desorbed powder before new hydrogenation in order to maintain favorable absorption characteristics.

Discussion

Dimagnesium iron(II) hydride, Mg_2FeH_6 , belongs to a structural class of ternary metal hydrides having the general composition M_2TH_n ($\text{M} =$ alkaline-earth or divalent rare-earth metal; $\text{T} =$ transition element of group 8, 9, or 10; $4 \leq n \leq 6$). Compounds of this class that have been reported so far are

T^8	T^9	T^{10}
$\text{Mg}_2\text{FeH}_6^a$	$\text{Ca}_2\text{RhH}_5^3$	$\text{Mg}_2\text{NiH}_4^{1,25,a}$
$\text{Ca}_2\text{RuH}_6^3$	$\text{Sr}_2\text{RhH}_5^3$	$(\text{Sr}_2\text{PdH}_4^{26})$
$\text{Sr}_2\text{RuH}_6^{3,a}$	$\text{Ca}_2\text{IrH}_5^3$	
$\text{Eu}_2\text{RuH}_6^4$	$\text{Sr}_2\text{IrH}_5^{3,23,a}$	
$\text{Yb}_2\text{RuH}_6^5$	$\text{Eu}_2\text{IrH}_5^{24}$	

^a Neutron diffraction data available.

Except for Sr_2PdH_4 , whose structure is unknown, all compounds crystallize with a CaF_2 -type metal atom arrangement containing interstitial H atoms. As the number of valence electrons of the T component is increased, the H content in the structure decreases and the H atom configuration around the T metal atoms changes from octahedral (Fe, Ru) to square pyramidal (Rh, Ir), and to presumably deformed square planar or tetrahedral (Ni). In those compounds that show nonoctahedral TH_n configurations, the H atoms are disordered at sufficiently high temperature and the crystals undergo a structural phase transition when the temperature is lowered (Sr_2IrH_5 cubic \rightarrow tetragonal,²³ $T_c \sim 190 \text{ K}$; Mg_2NiH_4 cubic \rightarrow monoclinic,¹² $T_c \approx 510 \text{ K}$). In all deuterides that were studied by neutron diffraction, the T-D distances were found

(20) Nakamoto, K. "Infra-Red and Raman Spectra of Inorganic and Coordination Compounds", 3rd ed.; Wiley-Interscience: New York, 1977; p 157.

(21) Chatt, J.; Hayter, R. G. *J. Chem. Soc.* **1961**, 5507.

(22) Mueller, W. M.; Blackledge, J. P.; Libowitz, G. G., Eds. "Metal Hydrides"; Academic Press: New York, 1968.

(23) Zhuang, J.; Hastings, J. M.; Corliss, L. M.; Bau, R.; Wei, C. Y.; Moyer, R. O., Jr. *J. Solid State Chem.* **1981**, *40*, 352.

(24) Moyer, R. O., Jr.; Lindsay, R. J. *Less-Common Met.* **1980**, *70*, P57.

(25) Reilly, J. J.; Wisswall, R. H., Jr. *Inorg. Chem.* **1968**, *7*, 2254.

(26) Stanitski, C.; Tanaka, J. *J. Solid State Chem.* **1972**, *4*, 331.

to be short and indicative of covalent bonding ($d(\text{T}-\text{D}) = 1.7 \text{ \AA}$ (Ir, Ru), $\sim 1.5 \text{ \AA}$ (Ni, Fe)), whereas the M-D distances were rather large and more typical for those in the ionic binary deuteride MD_2 . Thus, from a bonding point of view, one is led to consider the members of the M_2TH_n series as coordination compounds rather than as interstitial metal hydrides and to describe their structures as an array of divalent metal cations M^{2+} and complex anions TH_4^{4-} (T = Ni), TH_5^{4-} (T = Rh, Ir), or TH_6^{4-} (T = Fe, Ru). As pointed out previously¹ these complex anions appear to obey the 18-electron rule found for organometallic compounds, suggesting that the stability and maximal hydrogen content of this class of compounds are governed mainly by electronic factors. The discovery and properties of the new Fe-based representative Mg_2FeH_6 support this view. Its anion FeH_6^{4-} may be considered as a complex of low-spin t_{2g}^6 Fe(II) with six hydrido ligands and would be expected to have octahedral symmetry and a diamagnetic ground state, in agreement with the experimental data.

The Mg-D distances in Mg_2FeD_6 ($d(\text{Mg}-\text{D}) = 2.27 \text{ \AA}$) are close to those in β' - $\text{Mg}_2\text{NiD}_{3,9}$ (2.31 \AA at $280 \text{ }^\circ\text{C}$),¹ and they are both considerably greater than those in MgD_2 (1.95 \AA).²² These findings are consistent with the assumption of a more ionic character of the Mg-D bonds in the former compounds, as compared to that in MgD_2 . A Mg-H-Fe bridge bonding system similar to that found in BeH_2 or $\text{Al}(\text{BH}_4)_3$ can be excluded.

Octahedral coordination of Fe by hydrogen was also reported recently in $\text{FeH}_6\text{Mg}_4\text{X}_4(\text{THF})_8$ (X = halogen).¹⁸ The hydrido anion FeH_6^{4-} in this compound is surrounded by four Mg atoms which cap the faces of the H atom octahedron in a tetrahedral configuration. In Mg_2FeH_6 , by comparison, all octahedral faces are capped by Mg atoms which form a cubic configuration (Figure 3). The metal-hydrogen distances are

similar in both compounds ($\text{FeH}_6\text{Mg}_4\text{X}_4(\text{THF})_8$): $\bar{d}(\text{Fe}-\text{H}) = 1.69 \text{ \AA}$, $\bar{d}(\text{Mg}-\text{H}) = 2.06 \text{ \AA}$.

Finally we note that the hydrogen-to-metal weight ratio of Mg_2FeH_6 (5.4 wt %) is about 50% higher than that of Mg_2NiH_4 (3.6 wt %) and approaches that of MgH_2 (7.6 wt %). Moreover, its hydrogen content per unit volume (9.1×10^{22} atoms/cm³) exceeds by far those of Mg_2NiH_4 (5.4×10^{22}) and MgH_2 (6.5×10^{22}) and also those of the other known hydrogen storage media. With respect to thermal stability, Mg_2FeH_6 appears to be less promising for energy storage applications, mainly because of its high enthalpy of dissociation ($\Delta H_{\text{dis}} = 98 \text{ kJ/mol}$ of H_2), which exceeds those of Mg_2NiH_4 (64 kJ/mol of H_2)²³ and MgH_2 (74 kJ/mol of H_2).²²

In conclusion, we have prepared and characterized a new Fe-based ternary metal hydride having a favorable hydrogen-to-metal weight ratio and an exceptionally high density of hydrogen per unit volume. Structural analysis (X-ray and neutron powder diffraction) and spectroscopic measurements unambiguously indicate an octahedral H atom configuration for the Fe atoms in the crystal. The Mössbauer and infrared spectra of the compound are consistent with the presence of low-spin iron(II). No indication for a significant H deficiency or a homogeneity range could be detected within experimental error.

Acknowledgment. The financial support of the Swiss National Energy Research Foundation (NEFF) is gratefully acknowledged. J.J.D. and P.Z. are grateful to Dr. L. Schlapbach, P. Brack, and J. Osterwalder for help and hospitality during several stays at the ETH, Zürich. We thank Hans Hagemann for recording the Raman spectra. J.S. is grateful to the Swiss National Science Foundation for financial support.

Registry No. Mg_2FeH_6 , 89959-23-9; Mg_2FeD_6 , 89959-24-0.

Contribution from the Departments of Chemistry, Drexel University, Philadelphia, Pennsylvania 19104, and University of Virginia, Charlottesville, Virginia 22901

Spectroscopy and Structure of Thiolate and Thioether Complexes of Copper(II) and the Relationship of Their Redox Chemistry to That of Certain Copper Proteins

ANTHONY W. ADDISON,*^{1a} T. NAGESWARA RAO,^{1a} and EKKEHARD SINN^{1b}

Received August 9, 1983

Several complexes of copper and zinc(II) have been synthesized, with use of multidentate ligands entailing thiolate, phenolate, imine, and thioether donor atoms. The thioethers include tridentate and linear and macrocyclic tetra- and pentadentate ligands. The copper(II) complex of L-2, a potential N_2S (pyridyl, imine, thioether) donor, crystallizes in the space group $P2_1/c$, with cell constants $Z = 4$, $a = 9.212(7) \text{ \AA}$, $b = 14.439(6) \text{ \AA}$, $c = 15.117(9) \text{ \AA}$, $\beta = 95.60(6)^\circ$, $V = 2001 \text{ \AA}^3$, and $\rho_{\text{calcd}} = 1.748 \text{ g}\cdot\text{cm}^{-3}$. The structure, refined to $R_w = 7.4\%$, contains elongated pseudooctahedral Cu(II) ions, with the slightly distorted equator occupied by an H_2O and the nitrogen and sulfur atoms of the tridentate ligand. Perchlorates are weakly bound on the axial positions. Electron spin resonance, optical absorption, and UV difference spectroscopy have been used to delineate the coordination of the thiolate and thioether complexes in the solid state and in nonaqueous solution. Binding of the terminal thioether donors in these oligodentate ligands is solvent dependent. Coordination is optimized in MeNO_2 , but in certain of the complexes, the thioether sulfur is noncoordinated in dimethylformamide, where coordinative disproportionation occurs, as for $\text{Cu}(\text{L}-2)^{2+}$, which yields $\text{Cu}(\text{L}-2)_2^{2+}$. Monomeric thiolates have been prepared and characterized as having "normal" ESR parameters. The redox thermodynamics of the complexes has been examined by dc polarography and cyclic voltammetry. Most of the compounds generate stable Cu(I) states, the macrocyclic $\text{Cu}^1\text{N}_2\text{S}_2$ systems being notably so. The consequence of transforming a thiolato-copper complex to its thioether analogue is that the $E_{1/2}$ is elevated by about 0.5 V. This information is used to deduce the E° of a tetragonal $[\text{Cu}^1\text{N}_2\text{S}_2]^+$ moiety and thus comment on the possible roles of structural distortion and ligand transmutation at the type-1 active sites of copper proteins.

Introduction

Copper-sulfur interactions have attracted attention for some time, originally because of the intense colors associated with such systems^{2,3} and, more recently, because of the chain of

logic⁴⁻⁷ leading to the confirmation of cysteine thiolate and methionine thioether sulfur as active-site ligands to pseudo-

(1) (a) Drexel University. (b) University of Virginia.

(2) Klotz, I. M.; Urquhart, J. M.; Klotz, T. A.; Ayers, J. *J. Am. Chem. Soc.* **1955**, *77*, 1919.
(3) Klotz, I. M.; Czerlinski, G. H.; Fiess, H. A. *J. Am. Chem. Soc.* **1958**, *80*, 2920.